http://dx.doi.org/10.5012/bkcs.2012.33.8.2539

Performance Enhancement by Adaptation of Long Term Chronoamperometry in Direct Formic Acid Fuel Cell using Palladium Anode Catalyst

Yongchai Kwon, S. M. Baik,† Jonghee Han,‡,* and Jinsoo Kim†,*

Graduate School of Energy and Environment, Seoul National University of Science and Technology, Seoul 139-743, Korea
*†Department of Chemical Engimeering, Kyung Hee University, Gyeonggi-do 449-701, Korea. *E-mail: jkim21@khu.ac.kr*
*‡Fuel Cell Research Center, KIST, Seoul 130-650, Korea. *E-mail: jhan@kist.re.kr*
Received April 13, 2012, Accepted April 30, 2012

In the present study, we suggest a new way to reactivate performance of direct formic acid fuel cell (DFAFC) and explain its mechanism by employing electrochemical analyses like chronoamperometry (CA) and cyclic voltammogram (CV). For the evaluation of DFAFC perforamce, palladium (Pd) and platinum (Pt) are used as anode and cathode catalysts, respectively, and are applied to a Nafion membrane by catalyst-coated membrane spraying. After long DFAFC operation performed at 0.2 and 0.4 V and then CV test, DFAFC performance is better than its initial performance. It is attributed to dissolution of anode Pd into Pd^{2+}. By characterizations like TEM, Z-potential, CV and electrochemical impedance spectroscopy, it is evaluated that such dissolved Pd^{2+} ions lead to (1) increase in the electrochemically active surface by reduction in Pd particle size and its improved redistribution and (2) increment in the total oxidation charge by fast reaction rate of the Pd dissolution reaction.

Key Words : Direct formic acid fuel cell, Palladium recovery, Palladium dissolution, Electrochemical impedance spectroscopy

Introduction

Despite much progress made for establishing a baseline miniaturized fuel cell system and intensive efforts for making commercialization of the fuel cell system feasible, there are still many things to be addressed.[1-3] In a bid to make the miniaturized fuel cell system commercially viable, two main requirements should be met - excellent cell performance and long-lasting durability. Polymer electrolyte membrane fuel cells (PEMFCs) and direct methanol fuel cells (DMFCs) that utilize hydrogen and methanol as fuels have been continuously tested as the candidates for meeting the requirements.[4-6] However, in spite of such efforts, in PEMFCs, a high cost of hydrogen container and a low gas-phase energy density have prevented it from becoming a baseline fuel cell system, while in DMFCs, a slow rate of electrochemical methanol oxidation, a high fuel crossover rate, and an inherent toxicity have made its use hesitate.[7-9]

Unlike PEMFCs and DMFCs, direct formic acid fuel cells (DFAFCs) have recently drawn a comprehensive attention because of the expectation that the drawbacks of PEMFCs and DMFCs may be overcome. The DFAFCs use a liquid formic acid as fuel to produce electrical power. Electrochemical oxidation of formic acid is faster than that of methanol in DMFC due to simple molecular structure, and the DFAFCs provide higher electromotive force (EMF) than PEMFCs and DMFCs, while the fuel crossover rate in DFAFCs is lower than that in DMFCs. The lower crossover rate enables uses of thin polymer electrolyte membranes and highly concentrated liquid fuels in DFAFCs. The DFAFCs can be also operated at room temperature with low level of toxicity.[2,3,10,11]

For the operation of DFAFCs, platinum (Pt)-based catalysts have been used as an anode catalyst with partial successes like the achievement of feasible Pt bimetallic catalysts. However, as demands for the development of DFAFCs including high power density increased, there have been many attempts to discover more suitable catalyst materials, which can satisfy the power density and durability requirements.[12,13] Of the various candidates, palladium (Pd) has been considered the catalyst for replacing Pt catalyst.[2,3,10,14] The Pd catalyst enables not only improvement of the power density of DFAFC, but also operation at moderate temperature range (22-50 °C). The use of Pd as a catalyst for promoting electrooxidation of formic acid was initially reported by Ha *et al.*, and several research groups.[2,10,11,14] They evaluated affordability of the Pd catalyst for DFAFCs. According to their results, although the Pd catalyst led to the high power density in transient operation of DFAFCs, activity of the Pd catalyst reduced as the cell operation time is prolonged, affecting performance degradation of the DFAFCs.[10,14]

Due to that reason, it is critical to find solution about how to reactivate the Pd catalyst effectively during long DFAFC operation and how to maintain long term durability of the DFAFCs. Some research groups did related studies for elucidating the Pd reactivation mechanism of DFAFCs. Larsen *et al.*[10] and Yu *et al.*[15] applied a high anodic voltage of over 1.0 V to the DFAFCs and Yu *et al.* also executed cyclic potential scan tests in cell voltage range of 0.9 V ~ -0.3 V to recover the activity of Pd and performance of DFAFCs. Jung *et al.* [16] partially recovered activity of the Pd catalyst after the long operation by the application of higher anodic voltage than 1.0 V. However, all the previous reports

have shown that degree of the DFAFC performance recovered after the corresponding reactivation tests was no better than its initial performance.

In this paper, we suggest a way to gain better DFAFC performance than initial performance by carrying out both chronoamperometry (CA) under certain voltage range and cyclic voltammogram (CV). According to our results, dissolution and reallocation of Pd catalysts took place during the tests and such dissolved Pd^{2+} ions made a critical role in improving DFAFC performance by increasing electrochemically active surface (EAS) and total oxidation charge in Pd anode of the DFAFC single cell. For explaining the fact, several characterizations such as transmission electron microscope (TEM), Z-potential, CV and electrochemical impedance spectroscopy (EIS) were implemented.

Experimental

Preparation of Metal Catalysts and Electrodes. For cell testing, membrane electrode assemblies (MEAs) having an active area of 9.0 cm^2 were prepared using catalyst-coated membrane (CCM) spraying. The Pd black catalyst (High Surface Area, Sigma-Aldrich) and Pt black catalyst (HiSPEC™ 1000, Johnson Matthey) were used to prepare anode and cathode electrode. Their inks were obtained by dispersing the catalyst powders into Millipore water and 5% recast Nafion solution (1100EW, Solution Technology, Inc.). The inks were then air-sprayed onto both sides of a Nafion 115 membrane. The loadings of the Pd and Pt catalysts were 8 and 7 $mgcm^{-2}$, respectively. The membrane-deposited inks were then dried and carbon cloth diffusion layer (E-Tek) was added to cover the catalyst layers by hot-pressing for 1min at 130 °C with pressure of 250 kg cm^{-2}.[17]

DFAFC Single Cell Performance. The single cells were assembled with the prepared MEAs, installed at a fuel cell testing station (Fuel Cell Control System, CNL, Inc.) and pre-conditioned at a fixed potential of 0.6 V for 2 h. During the pre-conditioning, excessive hydrogen (200 sccm) and air (800 sccm) flows were supplied to anode and cathode, respectively. By continuous monitoring the cell current variation, the full activation of each MEA was achieved within 2 h. While the pre-conditioning was proceeded, single cell temperature was set to 80 °C and humidifier temperature was set to 75 °C for both gases, which corresponded to relative humidity of 81%. [18]

Cell polarization tests using formic acid and air were performed in the same fuel cell testing station as that used for pre-conditioning. 5 M formic acid was fed to anode at a constant feed rate (5 mL min^{-1}), while air (800 sccm) was fed to cathode. All fuel cell tests were conducted at 30 °C.

For intentional deactivation of DFAFC single cell, "time *vs.* current density" curve (chronoamperometry curve) was recorded for 20 h, remained voltage unchanged. During the tests, 5 M Formic acid was fed to anode at a constant feed rate (5 mL min^{-1}), while air (800 sccm) was fed to cathode. As the fixed voltages, four voltages – 0.2, 0.4, 0.6 and 0.8 V – were selected. All fuel cell tests were conducted at 30 °C.

Electrochemical Characterizations. CV tests were carried out to estimate EAS after 20 h-chronoamperometry test. For the tests, the voltage was scanned between 0.05 V and 1.2 V at a scan rate of 5 mV s^{-1}. De-ionized (DI) water was fed to anode (working electrode) at a constant feed rate (5 mL min^{-1}), while H_2 (400 sccm) was fed to cathode. Here, the Pt/H_2 combination in the cathode side of the cell acted as a dynamic hydrogen electrode (DHE) as well as a counter electrode.

EIS tests were performed to measure charge transfer resistance of the DFAFC. The frequency range used was from 10000 Hz to 0.005 Hz and the ac amplitude was 25 mV. 5 M Formic acid was fed to anode at a constant feed rate (5 mL min^{-1}), while H_2 (400 sccm) was fed to cathode.

Sizer (Photal, ELS-8000) that was one of accessories of Z-potential was used to investigate distribution and average particle group size of metal catalysts. For sample preparation for the sizer measurement, isopropanol and Millipore water solution were mixed as a ratio of 2 to 1with the total volume of 40 mL and then 0.02 g Pd powder was mingled to the solution. The mixture was dispersed by ultrasonic vibration under the condition of 2000 rpm for 1 min.

Results and Discussions

Pd Reactivation after Long Term Deactivation of DFAFC. To explore long term durability of DFAFC single cell and whether the DFAFC performance can be reactivated by long time operation, tests using DFAFC single cell were performed in three steps. In step 1, preconditioning of the DFAFC single cell was carried out and its polarization curve was measured (initial step). In step 2, CA test was performed for 20 h under pre-determined cell voltage. Lastly, in step 3, CV test was performed and final polarization curve was measured (reactivation step). As the fixed cell voltages for steps 2 and 3, 0.2, 0.4, 0.6, and 0.8 V were chosen.

Figure 1(a) shows the polarization curves of DFAFCs measured at initial reference step (step 1) and at reactivation step (step 3), respectively, under 4 different voltages and Figure 1(b) summarizes the maximum power densities (max PDs) of Figure 1(a) single cells. The four polarization curves measured at step 1 show similar max PDs irrespective of the fixed voltage, ensuring that the four DFAFC single cells are prepared in the same quality. On the other hand, the polarization curves measured at step 3 indicate a different pattern with applied fixed voltage. Namely, performances of DFAFC single cells that underwent the 20 h-CA and CV tests at 0.2 and 0.4 V (steps 2 and 3) were higher than those measured after initial reference step (step 1), whereas those of the DFAFCs that were measured at 0.6 and 0.8 V were lower than those measured after the step 1.

To find out possible reasons causing the effect of long time CA on DFAFC performance, several characterizations were carried out. Initially, CV curves were measured after each step under the four voltages and the summarized result is shown in Figure 2. In the Figure 2, when the fixed voltage was 0.6 and 0.8 V, background currents of CV curves

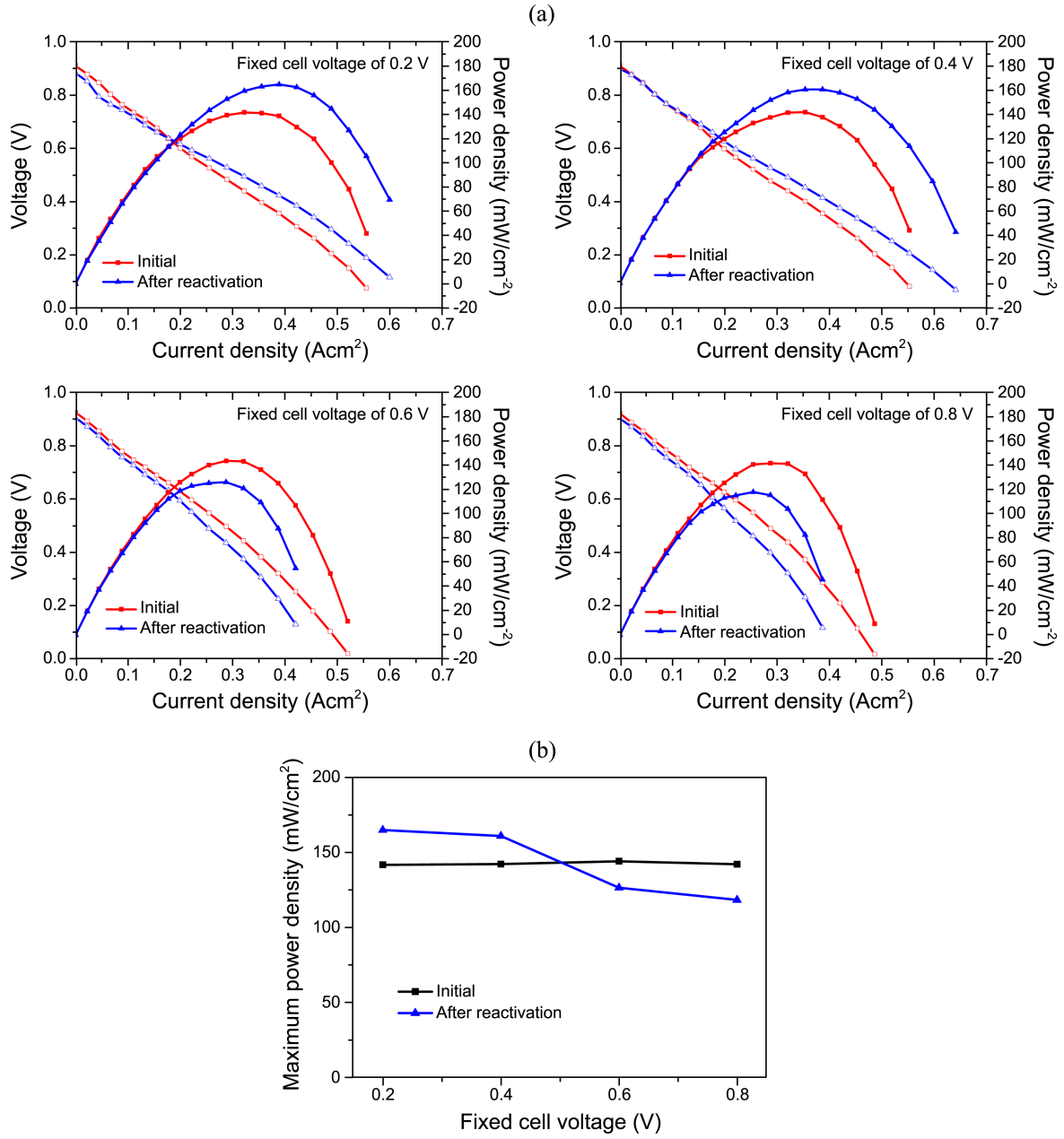

Figure 1. (a) Polarization curves of DFAFCs measured at initial reference step and at reactivation step, respectively, under 4 different fixed voltages. (b) The maximum power densities (max PDs) of Figure 1(a) single cells. For the tests, 5 M formic acid was fed to the anode at a constant feed rate (5 mLmin^{-1}), while air (800 sccm) was fed to the cathode. All fuel cell tests were conducted at 30 °C.

measured after step 1 were wider than those measured after step 3, indicating that EAS area of Pd catalyst reduced by the steps 2 and 3. Its area ratios (CV desorption area measured after step 3/CV desorption area measured after step 1) were 0.87 (at 0.6 V) and 0.71 (at 0.8 V), respectively. However, in fixed voltages of 0.2 and 0.4 V, the background currents of CV curves measured after step 1 were narrower than those measured after step 3, indicating that the EAS increased after the steps 2 and 3. Its area ratios were 1.04 (at 0.4 V) and 1.10 (at 0.2 V), respectively.

EIS tests were also carried out to evaluate the effect of charge transfer resistance (R_{ct}) on DFAFC performance (Figures 3(a) and 3(b)) and to investigate its correlation with CV result. Figure 3(a) shows Nyquist plots measured after steps 1 and 3, respectively, under the four different voltages, while Figure 3(b) summarized the R_{ct}s calculated from Figure 3(a). When the fixed voltages were 0.6 and 0.8 V, the R_{ct}s measured after step 3 were higher than those measured after step 1 (in 0.6 V, the R_{ct}s measured after steps 1 and 3 were 0.011 Ω cm^2 and 0.016 Ω cm^2, while in 0.8 V, those measured after steps 1 and 3 were 0.011 Ω cm^2 and 0.025 Ω cm^2), whereas the R_{ct}s measured after step 3 were lower than those measured after step 1 with 0.2 and 0.4 V (in 0.2 V, the R_{ct}s measured after steps 1 and 3 were 0.011 Ω cm^2 and 0.005 Ω cm^2, while in 0.4 V, those measured after steps 1 and 3 were 0.011 Ω cm^2 and 0.008 Ω cm^2). This EIS results

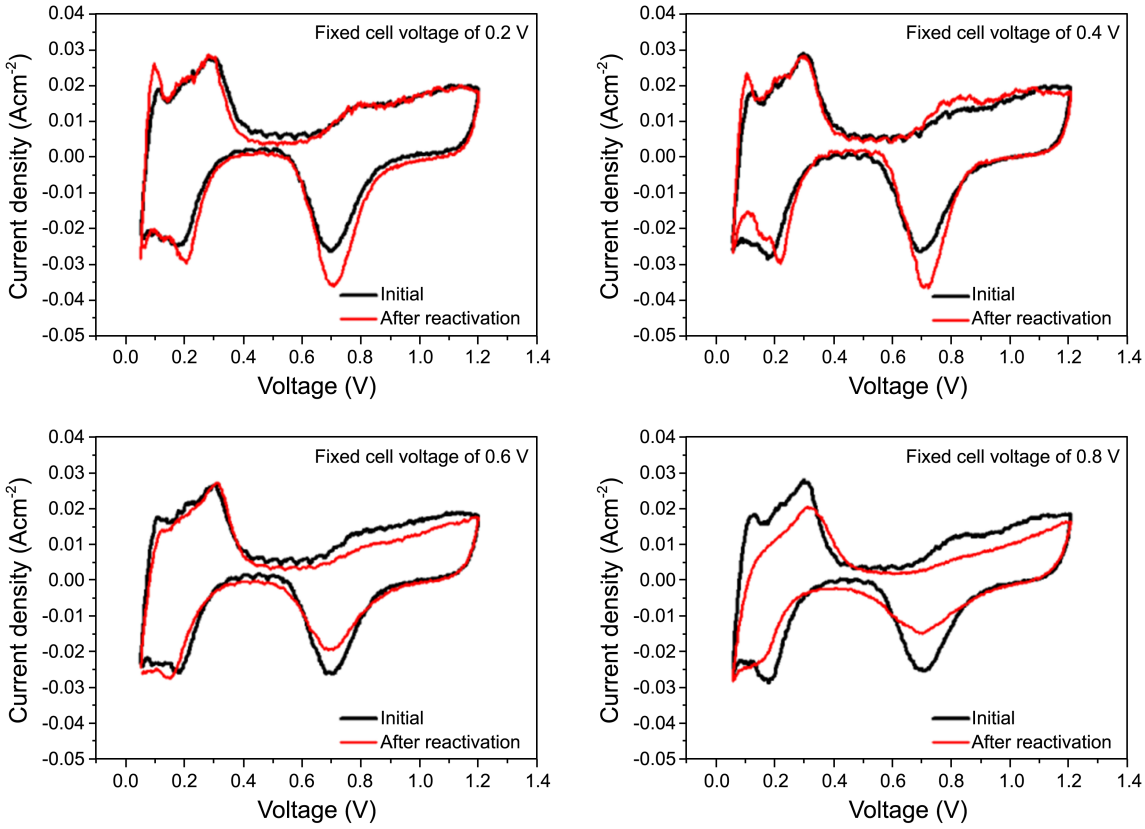

Figure 2. CV curves were measured after initial reference step and reactivation step, respectively, under 4 different fixed voltages. For the tests, the voltage was scanned between 0.05 V and 1.2 V at a scan rate of 5 mV s^{-1}. DI water was fed to anode (working electrode) at a constant feed rate (5 mL min^{-1}), while H_2 (400 sccm) was fed to cathode. All the tests were conducted at 30 °C.

confirm that with consecutive operation of steps 2 and 3, CA tests performed at voltages of 0.2 and 0.4 V result in increases in EAS and R_{ct} of anode side of DFAFC, while they decrease after the CA tests performed at 0.6 and 0.8 V.

Briefly, the CV and EIS results demonstrated that CA tests (step 2) performed in four different voltages affected the changes in EAS and R_{ct}. It is likely that the variances in anode Pd particle size and distribution are a feasible reason for such results. To investigate the effects of the Pd particle size and distribution on EAS and R_{ct}, they were measured after steps 1 and 3, respectively, using TEM and sizer of *z*-potential. As a reference, size of fresh Pd powder was also measured. The results were shown in Figures 4(a) and 4(b). In sizer results of the Figure 4(a), as the fixed voltage decreases, Pd particles are more finely dispersed and their particle size is getting smaller. Particularly, when the fixed voltage was 0.2 V, the Pd had the finest particle distribution and the smallest size. For instance, when they were measured after step 1 as a reference, their distribution range was 60-160 nm and average particle group size was ~96 nm. In DFAFC single cell that suffered CA and CV tests at 0.2 V, the Pd particle distribution reduced to 5.6-90 nm range and their average size reduced to ~26 nm. On the other hand, in the fixed voltage of 0.6 and 0.8 V, they were more aggregated and getting larger than those measured after step 1. In 0.6 and 0.8 V, the Pd particle distribution increased to 100-600 nm and 140-600 nm range and their particle size increased to ~217 nm and ~250 nm, respectively. TEM results of the Figure 4(b) also showed the similar tendency with sizer results, indicating that the lower fixed voltage was, the smaller size of Pd particles was.

Based on the Figures 1-4, it turns out that the long time CA tests leads to the changes in Pd particle size and distribution, followed by the changes in EAS and R_{ct} in Pd anode of DFAFC and eventually the change in the DFAFC performance.

To evaluate whether the long time CA tests also affect distribution and size of Pt particles on the cathode side, Pt particle size and distribution were measured after steps 1 and 3, respectively, under the four voltages by sizer and TEM, and the results were shown in Figure 5. Unlike Pd particles on anode side, there was no large difference in the Pt particle size and distribution irrespective of fixed voltage value. The Pt particles were equally dispersed to ~100 nm in all the tested samples. These results mean that anode Pd catalyst of DFAFC plays an important role in changes in DFAFC performance.

Pd Deactivation and Reactivation Mechanism Affecting DFAFC Cell Performance. From the result of above measurements, the best DFAFC performance was attained from the DFAFC single cell that underwent CA test at fixed voltage of 0.2 V. With subsequently implemented characterizations (*i.e.*, CV, EIS and spectroscopic inspections), it was demonstrated that the long time CA tests have influences on

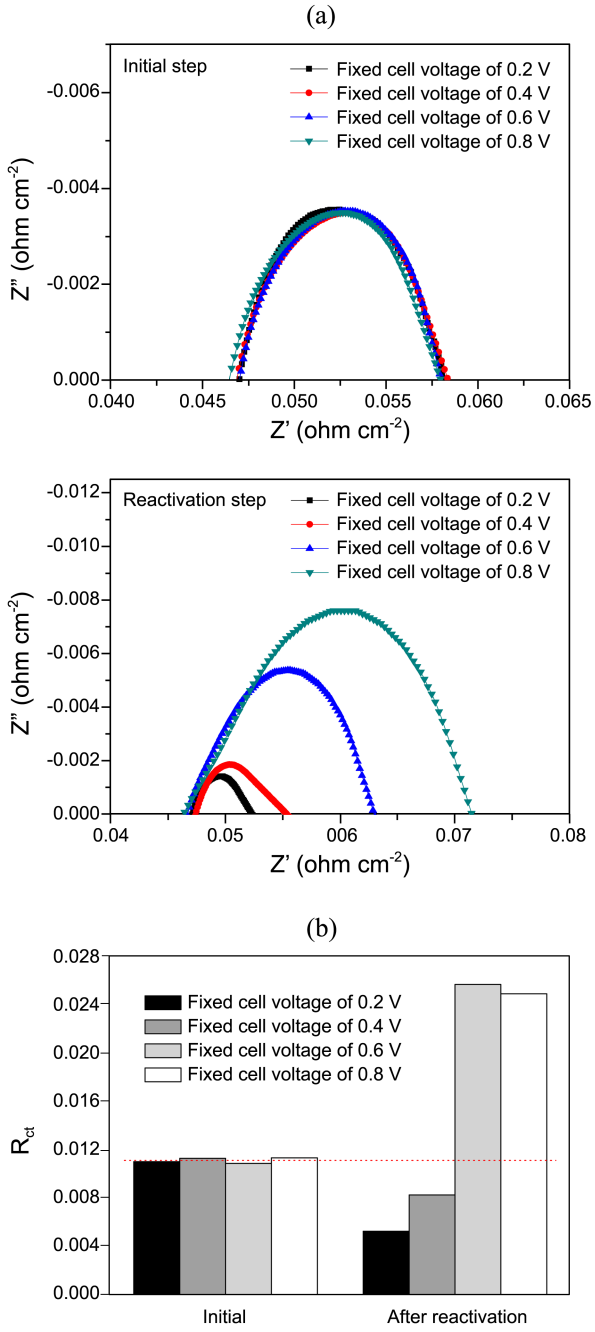

Figure 3. (a) EIS results measured at initial reference step and at reactivation step, respectively, under 4 differently fixed voltages. (b) Charge transfer resistances extracted from Figure 3(a) EIS tests in each step of 4 differently fixed voltages. For the tests, the frequency range used was from 10000 Hz to 0.005 Hz and the ac amplitude was 25 mV. 5 M Formic acid was fed to anode at a constant feed rate (5 mL min^{-1}), while H_2 (400 sccm) was fed to cathode. All fuel cell tests were conducted at 30 °C.

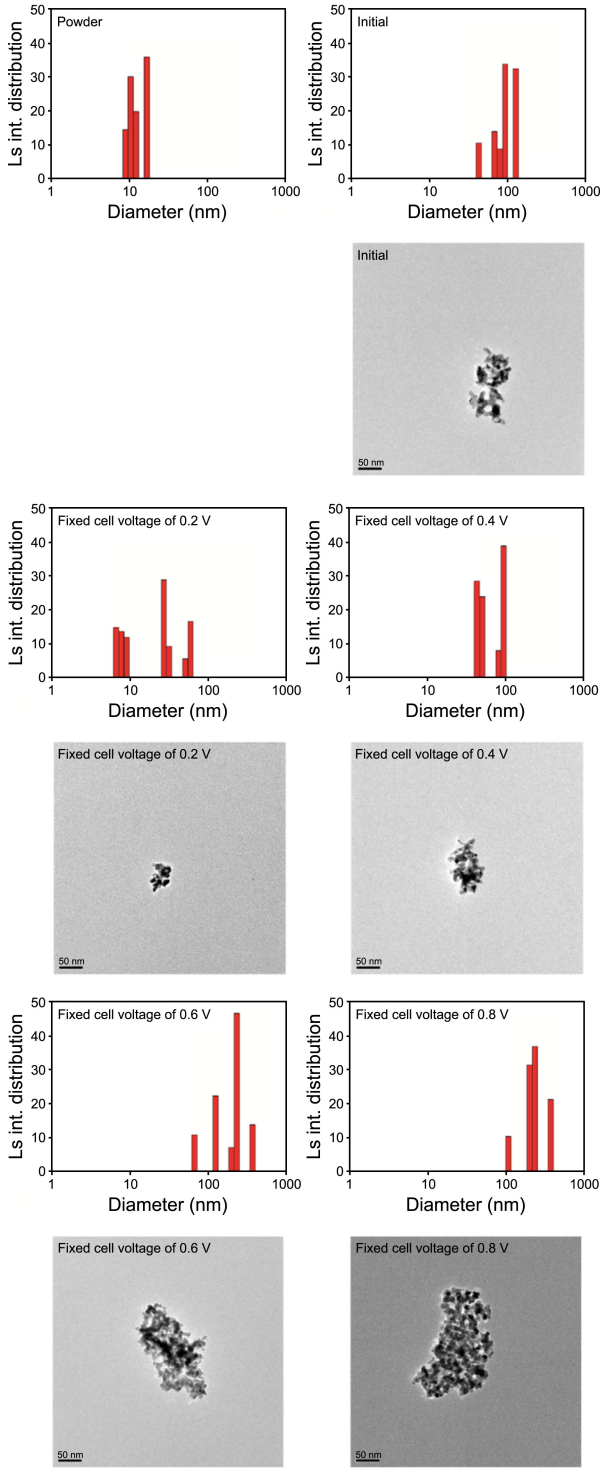

Figure 4. (a) Size and distribution of anode Pd particle measured by sizer after initial reference step and after reactivation step, respectively, under 4 different fixed voltages. Also, as a reference, those of fresh Pd power were measured. (b) TEM results, which were measured under the same condition as Figure 4(a) samples.

the changes in Pd particle size and distribution.

As a plausible scenario that explains the changes in size of Pd particles and their distribution, Pd dissolution occurring during the CA can be considered. According to previously published references, Pds are transformed as the following ways in certain voltage range.[19,20]

$$Pd \rightarrow Pd^{2+} + 2e^{-} \quad (1)$$

$$Pd^{2+} + HCOOH \rightarrow Pd + CO_2 + 2H^{+} \quad (2)$$

By the reactions (1) and (2), Pd particle is dissolved into

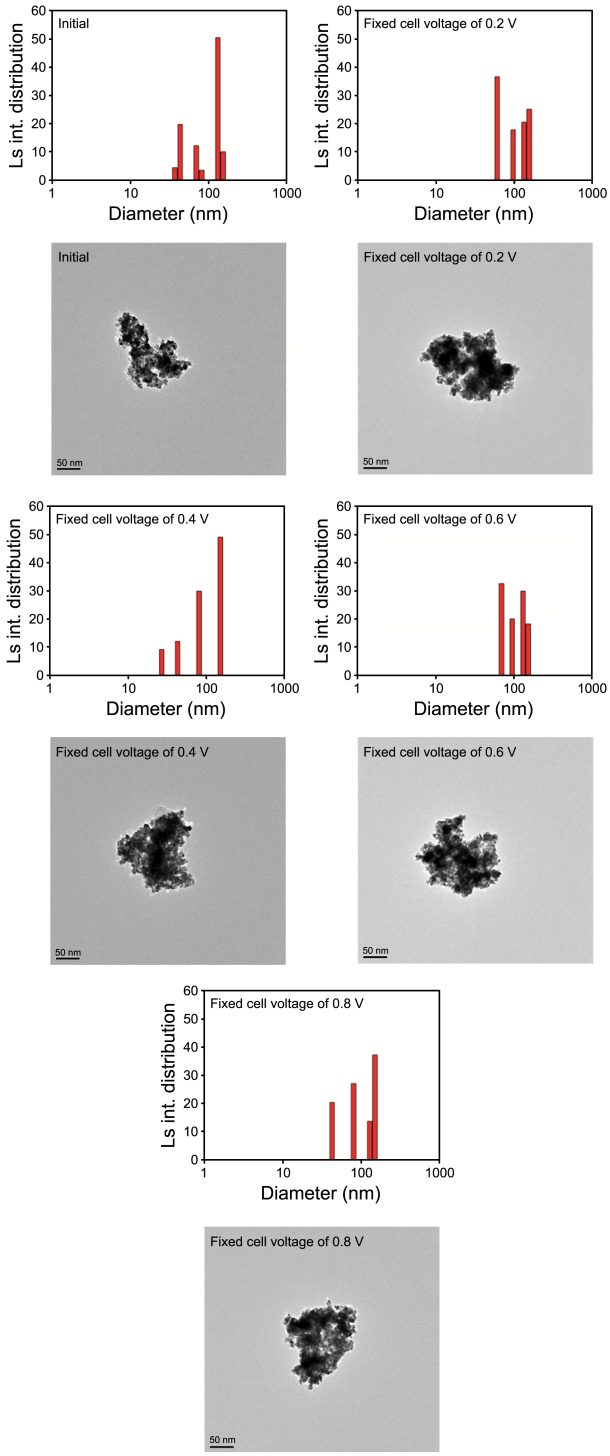

Figure 5. (a) Size and distribution of cathode Pt particle measured by sizer after initial reference step and after reactivation steps, respectively, under 4 different fixed voltages. (b) TEM results, which were measured under the same condition as Figure 5(a) samples.

Pd^{2+} ion and the Pd^{2+} ions react with formic acid. Transformation of Pd particle into Pd^{2+} ion can influence the DFAFC performance in two prospects. First, production of Pd^{2+} ions can reduce Pd particle size by existence of smaller Pd^{2+} ions and their uniform distribution by migration of the Pd^{2+} ions, followed by increases in EAS and DFAFC performance as shown in Figures 1-4.[19,21] Second, serial occurrence of reactions (1)-(2) gives rise to an increase in total oxidation charge. In the voltage range that the reactions (1)-(2) do not take place, the following multiple reactions are expected to occur.[21,22]

$$Pd + HCOOH \rightarrow Pd\text{-}COOH + H^+ + e^- \quad (3)$$

$$Pd + HCOOH + Pd\text{-}COOH \rightarrow Pd\text{-}C(OH)_2\text{-}Pd + CO_2 + H^+ + e^- \quad (4)$$

$$Pd\text{-}C(OH)_2\text{-}Pd \rightarrow 2Pd + CO_2 + 2H^+ + 2e^- \quad (5)$$

Because it is known that reaction (2) is faster process than reaction (5), indicating that reaction rate of reaction (2) is higher than that of reaction (5), more oxidation charges can be generated with reactions (1)-(2) than reactions (3)-(5).[19] It means that reaction (2) results in more total oxidation charge than reaction (5) during the same time. Indeed, the increase in total oxidation charge may well contribute to an improvement in DFAFC performance.

The Pd dissolution typically begins from ~0.7 V *vs*. DHE in anode of DFAFC.[23,24] This voltage is roughly equivalent to cell voltage of 0-0.2 V because the cathode voltage of DFAFC single cell is 0.8-0.9 V *vs.* DHE.[25,26] This cell voltage range of 0-0.2 V where Pd dissolution occurs corresponds to that of DFAFC showing best performance, proving that the Pd dissolution definitely affects the performance by improvement in EAS of Pd catalyst and increase in total oxidation charge of formic acid.

Conversely, if the cell voltage is far away from the 0-0.2 V (here, 0.6 and 0.8 V samples), two main factors will induce degradation in DFAFC performance. First, the slow reaction rate by reaction (5) that is responsible for the lack in Pd activity.[21] Second, the aggregation of Pd particles, which mainly occurs at initial stage of the CA test.[27] The former factor was confirmed by CV and EIS (see Figs. 2 and 3), while the latter factor was verified by Sizer and TEM (see Fig. 4)

Following the long time CA, CV and then DFAFC performance tests were performed (step 3) to investigate whether the DFAFC performance was regenerated. While water is fed to anode and air is fed to cathode for the tests, the following reactions take place at the anode.[19,28]

$$Pd + H_2O \rightarrow PdOH + H^+ + e^- \rightarrow PdO + 2H^+ + 2e^- \quad \text{(forward scan for anode catalyst)} \quad (6)$$

$$PdO + 2H^+ \rightarrow Pd^{2+} + H_2O \quad \text{(backward scan for anode catalyst)} \quad (7)$$

The DFAFC single cell that underwent CA test at 0.2 V showed the best performance after step 3 than those that underwent the test at 0.6 and 0.8 V. The DFAFC performance tested at 0.2 V is even better than that that did not undergo the test. As earlier explained, it is due to larger EAS and more total oxidation charges caused by dissolution of Pd into Pd^{2+} at the anode side of the DFAFC single cell.

Conclusions

Based on the results of this study, we suggest a way about how to interpret the reactivation mechanism in the DFAFC performance by using electrochemical experiments like CA and CV. From our test results, it was found performances of DFAFCs that underwent 20 h-CA test at the voltages of 0.2 and 0.4 V and CV test were better than those measured without the tests, whereas those that underwent the tests at 0.6 and 0.8 V did not reach the same level as those measured without the tests. By electrochemical characterizations, it was ascribed to dissolution of anode Pd catalysts into Pd^{2+}. Such dissolved Pd^{2+} resulted in increases in (1) EAS by the presence of smaller Pd^{2+} and its improved redistribution by migration of the Pd^{2+} and (2) oxidation charge production by fast reaction rate of the Pd dissolution reaction.

Acknowledgments. This work was supported by 2011 Seoul National University of Science and Technology research grant. The authors are grateful for the support from Seoul National University of Science and Technology.

References

1. Ha, S.; Larsen, R.; Masel, R. I. *J. Power Sources* **2005**, *144*, 28.
2. Yu, X.; Pickup, P. G. *J. Power Sources* **2008**, *182*, 124.
3. Yu, X.; Pickup, P. G. *J. Power Sources* **2009**, *187*, 493.
4. Acres, G. J. K. *J. Power Sources* **2001**, *100*, 60.
5. Winter, M.; Brodd, R. J. *Chem. Rev.* **2004**, *104*, 4245.
6. Choi, H.; Kim, J.; Kwon, Y.; Han, J. *J. Power Sources* **2010**, *195*, 160.
7. Neburchilov, V.; Martin, J.; Wang, H. J.; Zhang, J. J. *J. Power Sources* **2007**, *169*, 221.
8. Demirci, U. B. *J. Power Sources* **2007**, *169*, 239.
9. Song, S. Q.; Maragou, V.; Tsiakaras, P. *J. Fuel Cell Sci. Technol.* **2007**, *4*, 203.
10. Larsen, R.; Ha, S.; Zakzeski, J.; Masel, R. I. *J. Power Sources* **2006**, *157*, 78.
11. Zhang, L. L.; Lu, T. H.; Bao, J. C.; Tang, Y. W.; Li, C. *Electrochem. Commun.* **2006**, *8*, 1625.
12. Rice, C. A.; Ha, S.; Masel, R. I.; Wieckowski, A. *J. Power Sources* **2003**, *115*, 229.
13. Markovic, N. M.; Gasteiger, H. A.; Ross, P. N.; Jiang, X.; Villegas, I.; Weaver, M. J. *Electrochim. Acta* **1995**, *40*, 91.
14. Zhu, Y.; Khan, Z.; Masel, R. I. *J. Power Sources* **2005**, *139*, 15.
15. Yu, X.; Pickup, P. G. *J. Power Sources* **2008**, *182*, 124.
16. Jung, W. S.; Han, J.; Ha, S. *J Power Sources* **2007**, *173*, 53.
17. Baik, S. M.; Han, J.; Kim, J.; Kwon, Y. *Int J. Hydrogen Energy* **2011**, *36*, 14719.
18. Kim, S.; Han, J.; Kwon, Y.; Lee, K.-S.; Lim, T.-H.; Nam, S. W.; Jang, J. H. *Electrochim. Acta* **2011**, *56*, 7984.
19. Pavese, A.; Solis, V.; Giordano, M. C. *J. Electroanal. Chem.* **1988**, *245*, 145.
20. Gossner, K.; Mizera, E. *J. Electroanal. Chem.* **1979**, *98*, 37.
21. Pavese, A.; Solis, V.; Giordano, M. C. *Electrochim. Acta* **1987**, *32*, 1213.
22. Capon, A.; Parsons, R. *J. Electroanal. Chem.* **1973**, *44*, 239.
23. Rand, D. A. J.; Woods, R. J. *Electroanal. Chem.* **1972**, *35*, 209.
24. Bolzan, A.; Martins, M. E.; Arvia, A. J. *J. Electroanal. Chem.* **1983**, *157*, 339.
25. Li, G.; Pickup, P. G. *Electrochimica Acta* **2004**, *49*, 4119.
26. Uhm, S.; Chung, S. T.; Lee, J. *J. Power Sources* **2008**, *178*, 34.
27. Jung, W. S.; Han, J. H.; Yoon, S. P.; Nam, S. W.; Lim, T.-H.; Hong, S.-A. *J. Power Sources* **2011**, *196*, 4573.
28. Bolzan, A.; Martins, M. E.; Arvia, A. J. *J. Electroanal. Chem.* **1986**, *207*, 279.